

## RESEARCH ARTICLE

Hydration and glycogen affect  $T_1$  relaxation times of liver tissue

Ferenc E. Mózes<sup>1</sup>  | Ladislav Valkovič<sup>1,2</sup> | Michael Pavlides<sup>1,3,4</sup> |  
Matthew D. Robson<sup>1,5</sup> | Elizabeth M. Tunnicliffe<sup>1,4</sup> 

<sup>1</sup>The Oxford Centre for Clinical Magnetic Resonance Research (OCMR), University of Oxford, Oxford, UK

<sup>2</sup>Department of Imaging Methods, Institute of Measurement Science, Slovak Academy of Sciences, Bratislava, Slovakia

<sup>3</sup>Translational Gastroenterology Unit, University of Oxford, Oxford, UK

<sup>4</sup>Oxford NIHR Biomedical Research Centre, University of Oxford and Oxford Radcliffe Hospitals NHS Trust, Oxford, UK

<sup>5</sup>Perspectum, Gemini One, Oxford, UK

## Correspondence

Ferenc E. Mózes, The Oxford Centre for Clinical Magnetic Resonance Research (OCMR), University of Oxford, Level 0, John Radcliffe Hospital, Headley Way, Headington, Oxford, OX3 9DL, UK.  
Email: ferenc.mozes@cardiov.ox.ac.uk

## Funding information

NIHR Oxford Biomedical Research Centre, Grant/Award Number: #098436/Z/12/B; RDM Scholars Programme; Scatcherd European Scholarship; Sir Henry Dale Fellowship from the Royal Society and the Wellcome Trust; APVV, Grant/Award Number: #19-0032; Slovak Grant Agency VEGA, Grant/Award Number: #2/0003/20; National Institute for Health Research (NIHR) Oxford Biomedical Research Centre; UK Medical Research Council Doctoral Training Award, Grant/Award Number: MR/K501256/1

$T_1$  mapping is a useful tool for the assessment of patients with nonalcoholic fatty liver disease but still suffers from a large unexplained variance in healthy subjects. This study aims to characterize the potential effects of liver glycogen concentration and body hydration status on liver shortened modified Look-Locker inversion recovery (shMOLLI)  $T_1$  measurements. Eleven glycogen phantoms and 12 healthy volunteers (mean age: 31 years, three females) were scanned at 3 T using inversion recovery spin echo, multiple contrast spin echo (in phantoms), shMOLLI  $T_1$  mapping, multiple-echo spoiled gradient recalled echo and  $^{13}\text{C}$  spectroscopy (in healthy volunteers). Phantom  $r_1$  and  $r_2$  relaxivities were determined from measured  $T_1$  and  $T_2$  values. Participants underwent a series of five metabolic experiments to vary their glycogen concentration and hydration levels: feeding, food fasting, exercising, under-hydration, and rehydration. Descriptive statistics were calculated for shMOLLI  $T_1$ , inferior vena cava to aorta cross-sectional area ratio (IVC/Ao) as a marker of body hydration status, glycogen concentration,  $T_2^*$  and proton density fat fraction values. A linear mixed model for shMOLLI  $R_1$  was constructed to determine the effects of glycogen concentration and IVC/Ao ratio. The mean shMOLLI  $T_1$  after fasting was  $737 \pm 67$  ms. The mean within-subject change was  $80 \pm 45$  ms. The linear mixed model revealed a glycogen  $r_1$  relaxivity in volunteers ( $0.18 \text{ M}^{-1} \text{ s}^{-1}$ ,  $p = 0.03$ ) close to that determined in phantoms ( $0.28 \text{ M}^{-1} \text{ s}^{-1}$ ). A unit change in IVC/Ao ratio was associated with a drop of  $-0.113 \text{ s}^{-1}$  in  $R_1$  ( $p < 0.001$ ). This study demonstrated a dependence of liver shMOLLI  $T_1$  values on liver glycogen concentration and overall body hydration status. Interparticipant variation of hydration status should be minimized in future liver MRI studies. Additionally, caution is advised when interpreting liver  $T_1$  measurements in participants with excess liver glycogen.

## KEYWORDS

glycogen, hydration, liver, shMOLLI  $T_1$

**Abbreviations used:** Ao, aorta; bSSFP, balanced steady-state free precession; BW, bandwidth; CoV, coefficient of variation; FOV, field of view; GRAPPA, generalized autocalibrating partially parallel acquisitions; IDEAL, iterative decomposition of water and fat with echo asymmetry and least-squares estimation; IVC, inferior vena cava; LMM, linear mixed model; MCSE, multiple contrast spin echo; NAFLD, nonalcoholic fatty liver disease; NASH, nonalcoholic steatohepatitis; PDFF, proton density fat fraction; SE IR, spin echo inversion recovery; shMOLLI, shortened modified Look-Locker inversion recovery; TE, echo time; TE\*, acquisition delay (defined as the time between end of the excitation pulse and acquisition); TI, inversion time; TR, repetition time; TSE-IR, turbo spin echo inversion recovery.

This is an open access article under the terms of the Creative Commons Attribution License, which permits use, distribution and reproduction in any medium, provided the original work is properly cited.

© 2021 The Authors. *NMR in Biomedicine* published by John Wiley & Sons Ltd.

## 1 | INTRODUCTION

Nonalcoholic fatty liver disease (NAFLD) has recently seen a rise in prevalence both in Western countries and worldwide<sup>1</sup> as the manifestation of metabolic syndrome in the liver. Although it can be asymptomatic for prolonged periods of time and might not even progress to more severe stages, its natural progression includes the stages of accumulation of fat (termed simple steatosis), fatty inflammation of the liver (nonalcoholic steatohepatitis [NASH]) and later the additional development of fibrosis. In some patients, the disease may result in cirrhosis, liver failure and the development of hepatocellular carcinoma.

The current gold standard for the evaluation of NAFLD is liver biopsy. However, this carries risks of complications and mortality,<sup>2</sup> and suffers from high intraobserver and interobserver variability.<sup>3,4</sup> Therefore, the follow-up of patients undergoing either pharmaceutical interventions or lifestyle changes becomes difficult. As a result, the development of noninvasive methods that allow the diagnosis and prognosis of NAFLD remains an unmet need.

Liver proton  $T_1$  measured with the shortened modified Look-Locker inversion recovery (shMOLLI) method has been shown to be useful for characterizing disease and predicting disease outcomes.<sup>5–7</sup> While being clinically useful, the measured shMOLLI  $T_1$  is influenced by several factors: increased iron concentration,<sup>8</sup> static field inhomogeneities,<sup>9,10</sup> the presence of lipid deposition,<sup>9</sup> magnetization transfer<sup>11</sup> and sequence parameters.<sup>12,13</sup> However, even after correcting for all these factors, there is still a relatively high variance in the liver shMOLLI  $T_1$  of young, healthy individuals ( $\text{CoV}_{\text{liver}} = 6.83\%$ ).<sup>6</sup>

The liver synthesizes and breaks down glycogen in its role as an energy storage organ and therefore diurnal variation in hepatic glycogen content is expected. Gore et al. showed in a phantom study that increasing glycogen concentration shortens both  $T_1$  and  $T_2$  relaxation times,<sup>14</sup> an effect likely to be mediated by the viscosity of the glycogen macromolecule. Premenopausal women were suggested to have elevated liver  $T_1$  in comparison with postmenopausal women and men,<sup>15</sup> possibly due to hormonal changes that affect the overall fluid balance of the body. Hydration status influences  $T_1$  in the brain,<sup>16</sup> therefore it is reasonable to assume that it would also have an impact on liver  $T_1$  values, since the liver experiences daily fluid fluctuations. Glycogen and hydration status can be deliberately manipulated across a mixed cohort of healthy participants via simple interventions, such as fasting and exercise.

The aim of this study was thus to characterize the effects of liver glycogen concentration and body hydration status on liver shMOLLI  $T_1$  measurements in healthy individuals.

## 2 | METHODS

### 2.1 | Phantom experiments

Twelve phantoms were built with varying concentrations of oyster glycogen (Sigma Aldrich, UK) dissolved in deionized water. Phantoms were stored in 30-mL universal sample containers (King Scientific, UK). Glycogen was dissolved in 25 mL of water to form solutions of 0% to 11% by weight in steps of 1%.

Phantoms were scanned on the day of production in a 37°C water bath using a 3-T Prisma and a 1.5-T Avanto Fit scanner (Siemens Healthineers, Erlangen, Germany), both equipped with a 32-channel spine array coil and an 18-channel flexible coil. Turbo spin echo inversion recovery (TSE-IR) and multiple contrast spin echo (MCSE) images were collected at both field strengths. Sequence parameters for the TSE-IR were: FOV = 135 × 180 mm<sup>2</sup>, matrix 144 × 192, TI = 50, 100, 200, 400, 800, 1600, 2400 and 3200 ms, TR = 9000 ms, TE = 12 ms, slice thickness 6 mm, turbo factor 4. The MCSE sequence used the following parameters: FOV = 187 × 187 mm<sup>2</sup>, matrix 128 × 128, TR = 9000 ms, TE<sub>min</sub> = 15 ms, echo spacing 15 ms, number of echoes 32, slice thickness 6 mm. Sequence parameters of the TSE-IR and MCSE acquisitions were identical at 1.5 and 3 T. ShMOLLI  $T_1$  maps of the phantoms were collected using FOV = 332 × 248 mm<sup>2</sup> at 3 T and 360 × 270 mm<sup>2</sup> at 1.5 T, matrix size 192 × 144, TI<sub>min</sub> = 100 ms, TI<sub>increment</sub> = 80 ms, three inversion pulses (a gap of a 1-RR interval preceded the second and third inversion pulses), each followed by five, one and one readouts, respectively, acquired at intervals of 1000 ms, BW = 1300 Hz/px at 3 T and 900 Hz/px at 1.5 T, excitation FA = 35°, slice thickness 8 mm, GRAPPA acceleration factor 2. TR/TE = 2.41/1.05 ms was used at 3 T and TR/TE = 2.57/1.07 ms was used at 1.5 T. Single-shot images were reconstructed into a  $T_1$  map on the scanner console using the shMOLLI conditional fitting algorithm.<sup>17</sup> Individual TSE-IR images were fitted to Equation 1, while MCSE images were fitted to Equation 2 to obtain  $T_1$  and  $T_2$  maps, respectively.

$$S(TI) = S_0 \left( 1 - 2e^{-\frac{TI}{T_1}} \right) \quad (1)$$

$$S(TE) = S_0 e^{-\frac{TE}{T_2}} \quad (2)$$

In these equations  $S_0$  represents the signal at  $TI = 0$  ms and  $TE = 0$  ms, respectively.  $R_1$  ( $= 1/T_1$ , the longitudinal relaxation rate) and  $R_2$  ( $= 1/T_2$ , the transverse relaxation rate) values were fitted to Equation 3 to obtain longitudinal and transverse relaxivities of glycogen. Here,  $R_{10,20}$  are relaxation rates in the absence of glycogen,  $g$  is the concentration of glycogen (measured in mM), and  $r_{1,2}$  are relaxivity values of the glycogen (measured in  $\text{mM}^{-1} \text{s}^{-1}$ ).

$$R_{1,2} = R_{10,20} + r_{1,2}g. \quad (3)$$

## 2.2 | Human experiments

### 2.2.1 | Participant selection

Twelve healthy adults aged 20–50 years (three females), with a body mass index of 18–30  $\text{kg}/\text{m}^2$  and who were physically active (at the time of enrollment or in the past) were recruited. Exclusion criteria were as follows: self-reported kidney, liver, heart and lung disease or diabetes, regular alcohol consumption exceeding 14 units/week, the presence of metallic implants or pacemakers, pregnancy, or any other condition rendering the candidate unsuitable for an MRI examination. It has been shown previously that women actively using oral contraceptive pills also had elevated  $T_1$  values,<sup>18</sup> therefore we excluded women using oral contraceptives during the 3 months preceding enrollment. The study received ethical approval from the Central University Research Ethics Committee (reference R55780/RE001). All participants gave written informed consent.

### 2.2.2 | Study protocol

Every participant underwent five MRI examinations during the study over 3 days. On the first day participants were scanned 2.5 h after a standardized, high-calorie (1300 kcal), high-carbohydrate meal for dinner at 5 p.m., to measure liver proton  $T_1$  when glycogen levels are expected to be high. The hydration status was not manipulated (participants were in an euvoletic fed state – state 1). The next scan occurred on the following day at 8 a.m. after a 12-h long overnight fast, to measure  $T_1$  when glycogen levels are expected to be low (typically decreased by 40%–50% compared with baseline levels<sup>19</sup>; participants were in a low glycogen fasted state – state 2). Then participants immediately undertook a 2-h long stationary bicycle exercise session with an effort corresponding to a score of 6 on the modified Borg scale for perceived exertion.<sup>20</sup> After this activity, participants had a third scan, to measure  $T_1$  when glycogen is expected to be close to depletion (participants were in a depleted glycogen postexercise state – state 3).

Two to 6 days later there was another standardized, high-calorie (1300 kcal), high-carbohydrate meal consumed for dinner, a 12-h long overnight fast with the final 3 h water fasting, followed at 8 a.m. by a fourth scan, to measure  $T_1$  at moderately low amounts of glycogen and lower-than-normal hydration levels (participants were in a underhydrated state – state 4). The final scan was carried out on the same day at 10:20 a.m., after the consumption of 1.5 L of isotonic water, to measure  $T_1$  at a more moderate hydration level (participants were in a rehydrated state – state 5).

Participants were not asked to follow a predefined diet prior to enrolling in the study. The timing of individual study visits is depicted in Figure 1.

### 2.2.3 | MRI data acquisition and analysis

All in vivo MR acquisitions were performed on a 3-T Prisma scanner (Siemens Healthineers, Erlangen, Germany) and images of the liver were acquired in a single axial slice. shMOLLI acquisition parameters were: FOV =  $332 \times 248 \text{ mm}^2$ , matrix size  $192 \times 144$ , TR/TE = 2.41/1.05 ms,  $TI_{\min} = 100$  ms,  $TI_{\text{increment}} = 80$  ms, three inversion pulses (a gap of a 1-RR interval preceded the second and third inversion pulses), each followed by five, one and one readouts, respectively, synchronized to participants' ECG, BW = 1300 Hz/px, excitation FA = 35°, slice thickness 8 mm, GRAPPA acceleration factor 2. Single-shot images were reconstructed into a  $T_1$  map on the scanner console using the shMOLLI conditional fitting algorithm.<sup>17</sup> Proton density fat fraction (PDFF),  $B_0$  and  $T_2^*$  values were quantified using a multiple-echo spoiled GRE sequence with parameters: FOV =  $330 \times 248 \text{ mm}^2$ , matrix size  $128 \times 96$ , TR/TE = 17/0.94, 2.28, 3.60, 4.92, 6.24, 7.56, 8.88, 10.20, 11.52, 12.84, 14.16 and 15.48 ms, FA = 3°, phase-encoding direction anterior–posterior, BW = 1560 Hz/px, monopolar gradient readout scheme, and slice thickness 10 mm. PDFF,  $B_0$  and  $T_2^*$  values were obtained using the  $T_2^*$ -IDEAL algorithm.<sup>21,22</sup>

Glycogen concentration was measured using nonlocalized, natural abundance  $^{13}\text{C}$  spectroscopy with a dual-tuned flex surface coil (Rapid Biomedical, Rimpar, Germany) placed over the liver. Sequence parameters of the  $^{13}\text{C}$  spectroscopy acquisition were TR/TE\* = 400/0.6 ms, number

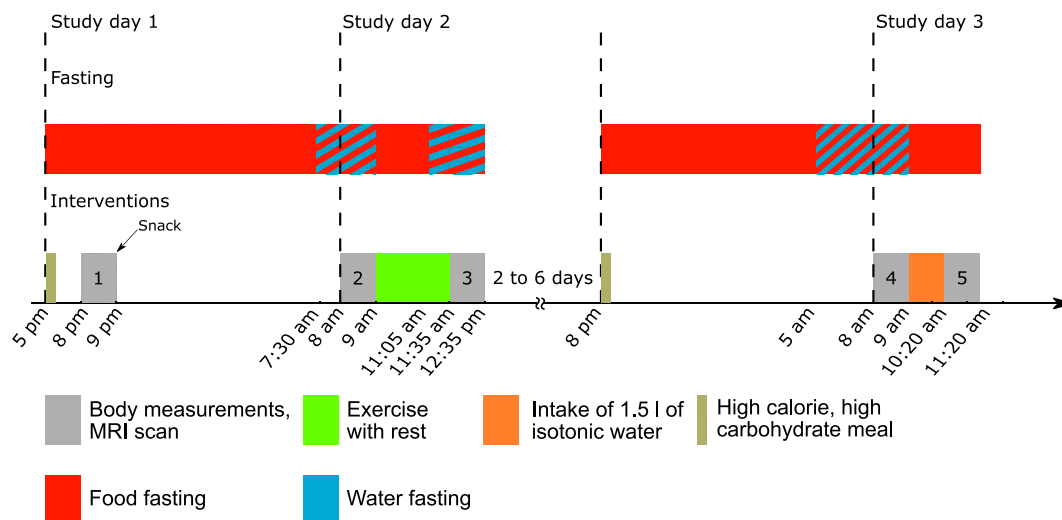


**FIGURE 1** Timing of study procedures for a single volunteer. Numbers in gray boxes (for MRI scans) correspond to the following physiological states: high glycogen, normal hydration - euvoletic fed (1), low glycogen - fasted (2), depleted glycogen - postexercise (3), low glycogen, low hydration - underhydrated (4), and low glycogen, high hydration - rehydrated (5), as described in the study protocol

of averages 2504, no decoupling, rectangular pulse of  $\tau_p = 1$  ms length, BW = 10 kHz, and vector size of 512 samples. The flip angle of the  $^{13}\text{C}$  spectroscopy acquisition was calibrated using a voltage sweep to achieve maximal signal intensity in a replacement phantom used for absolute quantification. No decoupling or nuclear Overhauser effect enhancement was available when the experiments were performed. A phantom replacement technique<sup>23</sup> was used for absolute quantification of liver glycogen concentration. For this, a phantom containing 300 mM of glycogen, 43 mM of sodium benzoate and 1.36 mM of  $\text{NiCl}_2$  was prepared in 1 L of phosphate-buffered solution. Spectra were fitted using the AMARES<sup>24</sup> algorithm in jMRUI<sup>25</sup> and resonance areas were corrected for variations in coil loading.<sup>23</sup> After removing all other peaks using the -Hankel-Lanczos singular value decomposition,<sup>26,27</sup> the resonances of the  $1\text{-}^{13}\text{C}$  doublet positioned at 97.8 and 103.2 ppm,<sup>28</sup> and the resonance of urea positioned at 167 ppm, were fitted to Lorentzian models. The  $1\text{-}^{13}\text{C}$  doublet resonances were constrained to have equal amplitudes.

Inferior vena cava to aorta cross-sectional area ratios (IVC/Ao) were considered the indicator of hydration status, similar to the IVC/Ao diameter ratio,<sup>29,30</sup> and were determined from the balanced steady-state free precession (bSSFP) image corresponding to the sixth inversion time of the shMOLLI experiment (in acquisition order).

Liver shMOLLI  $T_1$  values were determined as the average  $T_1$  over three ROIs placed in the liver such that they avoided the edge of the liver, visible vessels and bile ducts. Two ROIs were placed in the right lobe, one posteriorly and one anteriorly, and one ROI was placed in the left lobe. Since all participants were healthy volunteers and liver PDFF levels were expected to be below 5%, fat correction<sup>31</sup> was not performed. As off-resonance frequency variation over the liver was also expected to be minimal, frequency correction was not considered necessary either. Finally, shMOLLI  $T_1$  values were not corrected for iron, as all participants were expected to have normal levels of hepatic iron concentration and all changes in  $T_2^*$  measurements to be attributable to a glycogen dependence via the  $T_2$  component.

## 2.2.4 | Statistical analysis

The mean and standard deviation of shMOLLI  $T_1$ , glycogen concentration, IVC/Ao,  $T_2^*$  and PDFF were calculated for all five time points. The mean and standard deviation of within-participant change of these variables was also calculated.

Experimental data were fitted to a linear mixed model (LMM) to derive a relationship between shMOLLI  $R_1$  ( $= 1/T_1$ ) measurements, glycogen concentration and body hydration status. An LMM was chosen over a simple linear regression model due to the presence of repeated measures in the dataset introducing random baseline effects, along with time-varying covariates (glycogen concentration and hydration). The intrasubject correlation of shMOLLI  $R_1$  values was considered as a random effect, with an intercept for each participant determined by the model to accommodate for the different baseline  $R_1$ s. Equation 4 describes this LMM, where  $\beta_0$ ,  $\beta_1$  and  $\beta_2$  are the regressor coefficients for the intercept, glycogen concentration and IVC/Ao;  $(1|\text{subject})$  is the term for random effects due to intrasubject variation in  $R_1$  and  $\epsilon$  is the normally distributed error term with zero mean.

$$R_1 = \beta_0 + \beta_1[\text{glyco}] + \beta_2\text{IVC}/\text{Ao} + (1|\text{subject}) + \epsilon. \quad (4)$$

Paired, two-tailed t-tests with Holm's correction for multiple comparisons were used to test the significance of changes seen in shMOLLI  $T_1$ , glycogen concentration, hydration status,  $T_2^*$  and PDFF between fed and fasted, fasted and postexercise, and underhydrated and rehydrated states. For all statistical tests an  $\alpha = 0.05$  significance level was considered.

### 3 | RESULTS

#### 3.1 | Phantom experiments

Phantom  $R_1$  and  $R_2$  values showed linear dependence on glycogen concentration at both 1.5 and 3 T. Figure 2 presents the  $R_1$  and  $R_2$  maps reconstructed from spin echo experiments along with relaxivity fitting results at 3 T. The calculated longitudinal ( $r_1$ ) and transverse ( $r_2$ ) relaxivities are given in Table 1.

#### 3.2 | Human experiments

Details of the study cohort are included in Table 2. A typical baseline dataset is shown in Figure 3 with a  $T_1$  map, segmented inferior vena cava and aorta and a  $^{13}\text{C}$  spectrum with details of the glycogen doublet. Figure 3D also presents the evolution of the glycogen resonances during the

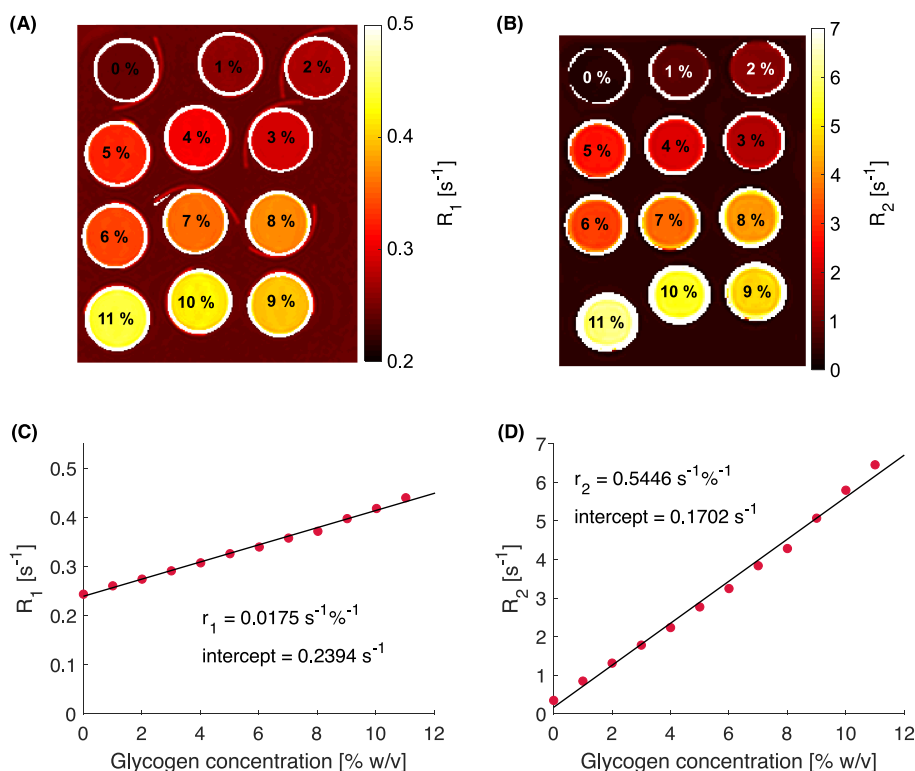


**FIGURE 2** Phantom  $R_1$  (A) and  $R_2$  (B) relaxation maps determined from spin echo experiments at 37°C and 3 T with vials labeled using their glycogen concentration. Having different glycogen concentrations across the vials allowed the estimation of  $r_1$  (C) and  $r_2$  (D) relaxivities

**TABLE 1** Experimentally determined longitudinal and transverse relaxivities of glycogen in phantoms at various field strengths

$B_0$ [T]	$r_1$ [% $^{-1}$ s $^{-1}$ ] (SE IR)	$r_1$ [M $^{-1}$ s $^{-1}$ ] (SE IR)	$r_1$ [% $^{-1}$ s $^{-1}$ ] (shMOLLI)	$r_1$ [M $^{-1}$ s $^{-1}$ ] (shMOLLI)	$r_2$ [% $^{-1}$ s $^{-1}$ ]	$r_2$ [M $^{-1}$ s $^{-1}$ ]
0.47*	0.055	0.880	-	-	0.217	3.472
1.5	0.025	0.392	0.024	0.384	0.322	5.152
3	0.018	0.280	0.018	0.280	0.545	8.720

\*denotes previously published data by Gore et al.<sup>14</sup>; no data on shMOLLI  $T_1$  is available from that study.

Relaxivities are provided both in units of % $^{-1}$  s $^{-1}$  and M $^{-1}$  s $^{-1}$  for convenience. We considered the relative molecular mass of glycogen to be 180 g/mol.

Variable	Mean ( $\pm$ SD, range) or n (%)
Age (years)	31 ( $\pm$ 7, 24–49)
Males (n)	8 (66.7%)
BMI ( $\text{kg}/\text{m}^2$ )	23.9 ( $\pm$ 2.4, 20.2–29.8*)
Weight (kg)	76.4 ( $\pm$ 13, 58.4–106.6)
Height (m)	1.78 ( $\pm$ 0.12, 1.63–2.09)

\*there was one athletic participant with a body mass index (BMI) close to  $30 \text{ kg}/\text{m}^2$ .

**TABLE 2** Characteristics of the study cohort (n = 12 participants)

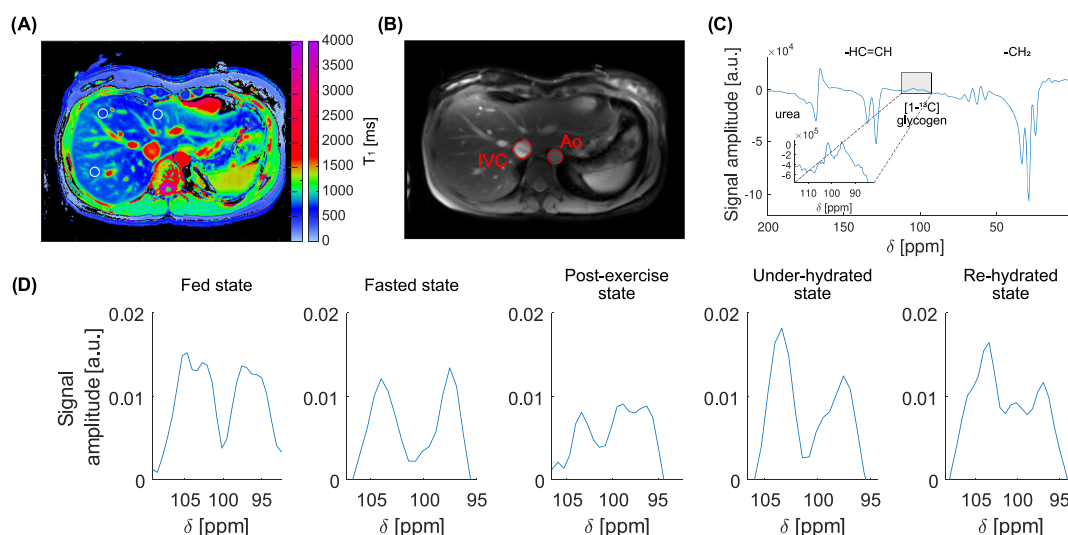


**FIGURE 3** Representative baseline data from the same volunteer: shMOLLI  $T_1$  map with three circular regions of interest (A); bSSFP image with contours of the inferior vena cava and of the aorta (B);  $^{13}\text{C}$  spectrum with an inset showing the glycogen (after phase correction) (C); and evolution of the glycogen signal over the five study visits (D)

**TABLE 3** Descriptive statistics of measured parameters at each time point averaged over all participants. Values are presented as mean (standard deviation)

Variable	Fed state	Low glycogen fasted state	Depleted glycogen postexercise state	Underhydrated state	Rehydrated state	Observed within-participant change <sup>a</sup>
Glycogen concentration (mM)	394 (170)	330 (180)*	181 (120)+++	324 (146)	305 (137)	242 (89)
IVC/Ao ratio	1.45 (0.65)	1.62 (0.55)	1.27 (0.66)+++	1.49 (0.58)	1.79 (0.61)++	0.66 (0.30)
shMOLLI $T_1$ (ms)	694 (51)	737 (67)***	714 (83)	729 (81)	745 (90)	80 (45)
$T_2^*$ (ms)	19 (3)	21 (3)*	20 (3)	21 (4)	22 (4)	5 (2)
PDFF (%)	1.78 (0.61)	1.34 (0.85)*	2.29 (0.84)++	2.12 (0.94)	1.93 (1.13)	1.59 (1.15)

\*, +, and † denote levels of significant difference compared with the fed, fasted and underhydrated state, respectively (\*  $p < 0.05$ , \*\*  $p < 0.01$ , \*\*\*  $p < 0.005$ ).

<sup>a</sup>Average of the difference between the maximum and minimum of the measured variables over all participants.

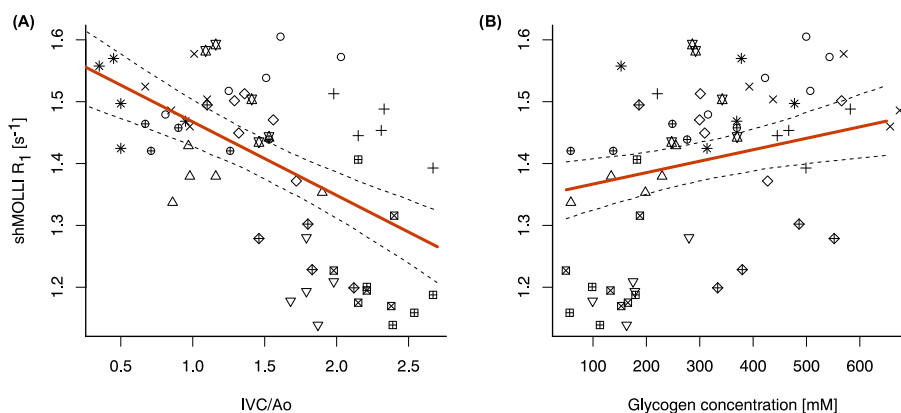
five study visits within one volunteer. PDFF was lower than 5% in each volunteer and  $T_2^*$  was reflective of normal hepatic iron concentrations. Descriptive statistics at all five time points are included in Table 3.

Table 4 presents the results of the LMM regression. As hypothesized, glycogen concentration had a positive effect while hydration status had a negative effect on liver  $R_1$ . Figure 4 illustrates the individual effects of IVC/Ao and glycogen concentration as determined by the LMM plotted alongside the raw data.

Glycogen concentration decreased between the fed and fasted states ( $p = 0.018$ , mean decrease: 61 mM, standard deviation: 76 mM) and between the fasted and postexercise states ( $p < 0.001$ , mean decrease: 152 mM, standard deviation: 94 mM). Hydration status as measured with the IVC/Ao ratio decreased between fasted and postexercise states ( $p < 0.001$ , mean decrease: 0.35, standard deviation: 0.19). Liver shMOLLI  $T_1$

**TABLE 4** Linear mixed model regression results ( $\beta$  represents a regressor coefficient, SE is the standard error) for a model considering all five time points

	$\beta$	SE	p value
Glycogen concentration ( $M^{-1} s^{-1}$ )	0.176	0.079	0.030
IVC/Ao ratio	−0.113	0.025	<0.001
Intercept ( $s^{-1}$ )	1.512	0.048	<0.001



**FIGURE 4** The individual effect of IVC/Ao (A) and glycogen concentration (B) on shMOLLI  $R_1$  values as determined from the linear mixed model. Of note is that on their own neither predictor can fully explain the variation in the underlying data. Each symbol corresponds to a single participant

values increased between the fed and fasted states ( $p < 0.001$ , mean increase: 43 ms, standard deviation: 36 ms). Differences between consecutive states for glycogen concentration, hydration status and liver proton  $T_1$  are shown in Figure 5.

Although the IVC/Ao ratio increased between the underhydrated and rehydrated states ( $p = 0.003$ , mean increase: 0.302, standard deviation: 0.276), the increase seen in liver shMOLLI  $T_1$  between the two states did not reach statistical significance.

## 4 | DISCUSSION

This study investigated the dependence of liver shMOLLI  $T_1$  on body hydration status and on liver glycogen concentration. Our in vivo results are in agreement with what has been previously reported in the literature in glycogen phantoms: a decrease in glycogen concentration led to a longer liver shMOLLI  $T_1$ ; in addition, we have also found that a decrease in IVC/Ao ratio led to a shorter liver shMOLLI  $T_1$ . In contrast to other influencing factors of shMOLLI  $T_1$  measurements of the liver (e.g. fat and iron accumulation<sup>8,9</sup>), variation in both glycogen concentration and hydration status results in an intrinsic change of tissue  $T_1$ , which would also be observed when using other  $T_1$  measurement methods.

Previously reported work showed equivocal effects of glycogen on  $T_1$  and  $T_2$  relaxation time variation in vivo.<sup>32,33</sup> However, these studies did not simultaneously consider the effect of blood volume variation or tissue water content. The multivariate model we used in this study allows for the separation and quantification of the opposite effects of glycogen and hydration status. These competing effects account for the lack of statistical significance when t-tests are used for comparison of shMOLLI  $T_1$  between, for example, the dehydrated and rehydrated time points.

The relaxivity of glycogen in the liver as predicted by our LMM is close to the relaxivity determined in phantoms, but the two values do not agree perfectly. The difference between the two values may be due to our limited understanding of the effect of exercise<sup>34</sup> on liver physiology, and thus  $T_1$  measurements. As no spatial localization was used for  $^{13}C$  MRS, our glycogen measurements may be also slightly biased by the glycogen signal originating from participants' chest walls, especially in the case of more athletic participants with thicker chest walls. As muscle generally has a lower concentration of glycogen than liver,<sup>35</sup> liver glycogen concentrations could be underestimated in the presence of a thicker layer of chest muscle. This may provide some explanation for the relatively wide range of absolute glycogen concentrations recorded and some further explanation as to why the calculated in vivo relaxivity did not completely match the phantom experiments.

Metabolic interventions were designed to push participants into extreme conditions in an attempt to determine maximal changes in the measured parameters in a short space of time. However, changes of this magnitude are possible between different disease states. For example, patients with diabetes can have a baseline fasting liver glycogen concentration as much as approximately 30% lower than patients without diabetes,<sup>36</sup> while in our study an average decrease of 54% was recorded between the fed and fasted states. The observed mean increase in shMOLLI  $T_1$  of the liver between the fed and fasted states of 43 ms implies a far larger relaxivity for glycogen of  $1.38 M^{-1} s^{-1}$  than either the



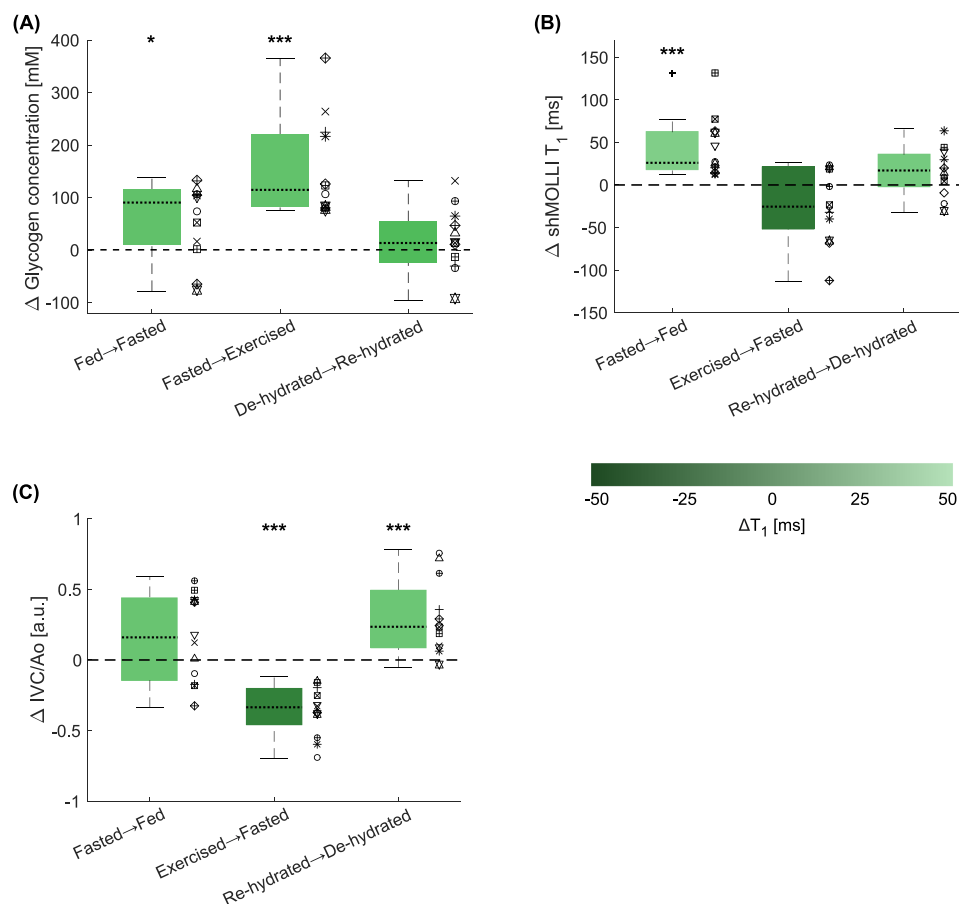


**FIGURE 5** Change in glycogen concentration (A), liver T<sub>1</sub> (B) and hydration status (C) between the fasted and fed, postexercise and fasted, and rehydrated and dehydrated states. Box plots are color-coded by the effect size of the change on liver T<sub>1</sub> measurements. It should be noted that while changes in glycogen concentration and hydration status were significantly different from zero, corresponding changes in liver T<sub>1</sub> measurements did not differ significantly from zero due to the opposing effects of glycogen and hydration. \**p* < 0.05, \*\*\* *p* < 0.005

phantom or LMM are consistent with. Given the range of glycogen concentrations and IVC/Ao ratios seen in our study and the LMM results, glycogen variation would lead to changes of up to 22 ms and hydration changes of up to 41 ms in T<sub>1</sub>. This implies that there are additional, perhaps diurnal, effects on liver proton T<sub>1</sub>, other than glycogen and hydration, which our study was not designed to probe.

Our results suggest that most variations in T<sub>1</sub> due to glycogen in healthy volunteers or in patients with common diseases like diabetes<sup>36</sup> are within the single-session repeatability ranges previously reported for liver proton T<sub>1</sub>.<sup>37</sup> However, patients with glycogen storage disease, where liver glycogen can be increased to three times its usual value,<sup>38</sup> will have a native T<sub>1</sub> that is lower by approximately 60 ms. Hydration is not usually controlled in our local scanning protocols. However, our data suggest that it may be more important to control hydration than food intake. Given a 4-h fasting period is often imposed prior to research study visits, it is important to ensure that subjects are not replacing food intake with fluid intake. In longitudinal studies, it is possible to measure IVC/Ao ratio within the same subject to determine whether hydration status is consistent between scans.

The results of this study may be limited by the small number of participants, as well as the lack of direct measurement of hydration status, although it is unclear what biomarker to consider as a reference standard.<sup>39,40</sup> Biomarkers like blood osmolality and jugular vein pressure have been proven to be good indicators of dehydration, but they are not routinely used as markers of hydration status.

In conclusion, we have shown a clear dependence of liver proton T<sub>1</sub> values on body hydration status and glycogen concentration. While the glycogen-induced variation in liver T<sub>1</sub> suggested by our LMM is within the single-session repeatability T<sub>1</sub> range, these relationships should be considered when designing new imaging studies. In particular, T<sub>1</sub> mapping should be avoided in patients with excess glycogen in their liver due to glycogen storage disease. Additionally, variations in participants' hydration status should also be minimized as part of the preparation for MRI scans, for example, by imposing restrictions on the amount of liquid intake, such as consuming no more than 0.5 L of water 1 h before an MRI scan.



## ACKNOWLEDGEMENTS

FEM was funded by a UK Medical Research Council Doctoral Training Award (MR/K501256/1), a Scatcherd European Scholarship and the RDM Scholars Programme. EMT received funding from the National Institute for Health Research (NIHR) Oxford Biomedical Research Centre. LV was funded by a Sir Henry Dale Fellowship (grant #098436/Z/12/B) from the Royal Society and the Wellcome Trust. The support of the Slovak Grant Agency VEGA (grant #2/0003/20) and APVV (grant #19-0032) is also acknowledged. The views expressed are those of the authors and not necessarily those of the NHS, the NIHR or the Department of Health.

## CONFLICT OF INTEREST

EMT is an inventor on patents related to corrected  $T_1$  ( $cT_1$ ) and its use for the assessment of liver disease, and is a minority shareholder in Perspectum, who have licensed these patents. MDR is founder and CTO of Perspectum.

## DATA AVAILABILITY STATEMENT

The data that support the findings of this study are available from the corresponding author upon reasonable request.

## ORCID

Ferenc E. Mózes  <https://orcid.org/0000-0002-1361-4349>

Elizabeth M. Tunnicliffe  <https://orcid.org/0000-0002-6945-5201>

## REFERENCES

1. Younossi ZM, Koenig AB, Abdelatif D, Fazel Y, Henry L, Wymer M. Global epidemiology of nonalcoholic fatty liver disease-Meta-analytic assessment of prevalence, incidence, and outcomes. *Hepatology*. 2016;64(1):73-84.
2. Thampanitchawong P, Piratvisuth T. Liver biopsy: complications and risk factors. *World J Gastroenterol*. 1999;5(4):301-304.
3. Standish RA, Cholongitas E, Dhillon A, Burroughs AK, Dhillon AP. An appraisal of the histopathological assessment of liver fibrosis. *Gut*. 2006;55(4):569-578.
4. Hall AR, Green AC, Luong T-V, Burroughs AK, Wyatt J, Dhillon AP. The use of guideline images to improve histological estimation of hepatic steatosis. *Liver Int*. 2014;34(9):1414-1427.
5. Pavlides M, Banerjee R, Sellwood J, et al. Multiparametric magnetic resonance imaging predicts clinical outcomes in patients with chronic liver disease. *J Hepatol*. 2016;64(2):308-315.
6. Banerjee R, Pavlides M, Tunnicliffe EM, et al. Multiparametric magnetic resonance for the non-invasive diagnosis of liver disease. *J Hepatol*. 2014;60(1):69-77.
7. Pavlides M, Banerjee R, Tunnicliffe EM, et al. Multiparametric magnetic resonance imaging for the assessment of non-alcoholic fatty liver disease severity. *Liver Int*. 2017;37(7):1065-1073.
8. Tunnicliffe EM, Banerjee R, Pavlides M, Neubauer S, Robson MD. A model for hepatic fibrosis: the competing effects of cell loss and iron on shortened modified Look-Locker inversion recovery  $T_1$  (shMOLLI- $T_1$ ) in the liver. *J Magn Reson Imaging*. 2017;45(2):450-462.
9. Mozes FE, Tunnicliffe EM, Pavlides M, Robson MD. Influence of fat on liver  $T_1$  measurements using modified Look-Locker inversion recovery (MOLLI) methods at 3T. *J Magn Reson Imaging*. 2016;44(1):105-111.
10. Kellman P, Herzka DA, Arai AE, Hansen MS. Influence of Off-resonance in myocardial  $T_1$ -mapping using SSFP based MOLLI method. *J Cardiovasc Magn Reson*. 2013;15(1):63.
11. Robson MD, Piechnik SK, Tunnicliffe EM, Neubauer S.  $T_1$  measurements in the human myocardium: The effects of magnetization transfer on the SASHA and MOLLI sequences. *Magn Reson Med*. 2013;67(3):664-670.
12. Kellman P, Bandettini WP, Mancini C, Hammer-Hansen S, Hansen MS, Arai AE. Characterization of myocardial  $T_1$ -mapping bias caused by intramyocardial fat in inversion recovery and saturation recovery techniques. *J Cardiovasc Magn Reson*. 2015;17(1):33.
13. Mózes FE, Tunnicliffe EM, Robson MD. The echo time of balanced steady-state free precession readouts modulates the influence of fat on MOLLI  $T_1$  measurements. In: *Proceedings of the International Society for Magnetic Resonance in Medicine* 27; 2019:4975.
14. Gore JC, Brown MS, Mizumoto CT, Armitage IM. Influence of glycogen on water proton relaxation times. *Magn Reson Med*. 1986;3(3):463-466.
15. Mojtahed A, Kelly CJ, Herlihy AH, et al. Reference range of liver corrected  $T_1$  values in a population at low risk for fatty liver disease—a UK Biobank sub-study, with an appendix of interesting cases. *Abdom Radiol*. 2018;44(1):1-13.
16. Meyers SM, Tam R, Lee JS, et al. Does hydration status affect MRI measures of brain volume or water content? *J Magn Reson Imaging*. 2016;44(2):296-304.
17. Piechnik SK, Ferreira VM, Dall'Armellina E, et al. Shortened Modified Look-Locker Inversion recovery (ShMOLLI) for clinical myocardial  $T_1$ -mapping at 1.5 and 3 T within a 9 heartbeat breathhold. *J Cardiovasc Magn Reson*. 2010;12(1):69.
18. Richards MA, Webb JAW, Jewell SE, Gregory WM, Reznick RH. In vivo measurement of spin lattice relaxation time ( $T_1$ ) of liver in healthy volunteers: the effects of age, sex and oral contraceptive usage. *Br J Radiol*. 1988;61(721):34-37.
19. Rothman D, Magnusson I, Katz L, Shulman R, Shulman G. Quantitation of hepatic glycogenolysis and gluconeogenesis in fasting humans with  $^{13}\text{C}$  NMR. *Science*. 1991;254(5031):573-576.
20. Borg GA. Psychophysical bases of perceived exertion. *Med Sci Sports Exerc*. 1982;14(5):377-381.
21. Hernando D, Kellman P, Halder JP, Liang Z-P. Robust water/fat separation in the presence of large field inhomogeneities using a graph cut algorithm. *Magn Reson Med*. 2010;63(1):79-90.
22. Hernando D, Kühn J-P, Mensel B, et al.  $R_2^*$  estimation using “in-phase” echoes in the presence of fat: The effects of complex spectrum of fat. *J Magn Reson Imaging*. 2013;37(3):717-726.

23. Lei H, Morgenthaler F, Yue T, Gruetter R. Direct validation of in vivo localized  $^{13}\text{C}$  MRS measurements of brain glycogen. *Magn Reson Med*. 2007; 57(2):243-248.
24. Vanhamme L, van den Boogaart A, Van Huffel S. Improved method for accurate and efficient quantification of MRS data with use of prior knowledge. *J Magn Reson*. 1997;129(1):35-43.
25. Naressi A, Couturier C, Devos JM, et al. Java-based graphical user interface for the MRUI quantitation package. *Magma Magn Reson Mater Phys Biol Med*. 2001;12(2-3):141-152.
26. Pijnappel WW, van den Boogaart A, de Beer R, van Ormondt D. SVD-based quantification of magnetic resonance signals. *J Magn Reson*. 1992;97(1): 122-134.
27. Vanhamme L, Fierro RD, Van Huffel S, De Beer R. Fast removal of residual water in proton spectra. *J Magn Reson*. 1998;132(2):197-203.
28. Avison MJ, Rothman DL, Nadel E, Shulman RG. Detection of human muscle glycogen by natural abundance  $^{13}\text{C}$  NMR. *Proc Natl Acad Sci U S A*. 1988; 85(5):1634-1636.
29. Kwon H, Lee J, Kim K, Kwak Y, Kim D. Measurement of inferior vena cava and aorta with bedside ultrasound to assess degree of dehydration in children. *Crit Ultrasound J*. 2015;7(Suppl 1):A23.
30. Durajska K, Januszkiewicz E, Szmygel Ł, Kosiak W. Inferior vena cava/aorta diameter index in the assessment of the body fluid status - a comparative study of measurements performed by experienced and inexperienced examiners in a group of young adults. *J Ultrason*. 2014;14(58):273-279.
31. Mozes FE, Tunnicliffe EM, Moolla A, et al. Mapping tissue water T1 in the liver using the MOLLI T1 method in the presence of fat, iron and B0 inhomogeneity. *NMR Biomed*. 2019;32(2):e4030.
32. Price TB, Gore JC. Effect of muscle glycogen content on exercise-induced changes in muscle T2 times. *J Appl Physiol*. 1998;84(4):1178-1184.
33. Sostman D, Zoghbi S, Gore J. Temporal fluctuations in proton relaxation times. *Magn Reson Imaging*. 1986;4(6):479-483.
34. Trefts E, Williams AS, Wasserman DH. Exercise and the regulation of hepatic metabolism. *Prog Mol Biol Transl Sci*. 2015;135:203-225.
35. Hearnis M, Hammond K, Fell J, Morton J. Regulation of muscle glycogen metabolism during exercise: implications for endurance performance and training adaptations. *Nutrients*. 2018;10(3):298.
36. Magnusson I, Rothman DL, Katz LD, Shulman RG, Shulman GI. Increased rate of gluconeogenesis in type II diabetes mellitus. A  $^{13}\text{C}$  nuclear magnetic resonance study. *J Clin Invest*. 1992;90(4):1323-1327.
37. Bachtar V, Kelly MD, Wilman HR, et al. Repeatability and reproducibility of multiparametric magnetic resonance imaging of the liver. *PLoS One*. 2019; 14(4):e0214921.
38. Stevens AN, Richard AI, Peter GM, Griffiths JR. Detection of glycogen in a glycogen storage disease by  $^{13}\text{C}$  nuclear magnetic resonance. *FEBS Lett*. 1982;150(2):489-493.
39. Armstrong LE, Maughan RJ, Senay LC, Shirreffs SM. Limitations to the use of plasma osmolality as a hydration biomarker. *Am J Clin Nutr*. 2013;98(2): 503-504.
40. Perrier E, Rondeau P, Poupin M, et al. Relation between urinary hydration biomarkers and total fluid intake in healthy adults. *Eur J Clin Nutr*. 2013; 67(9):939-943.

**How to cite this article:** Mózes FE, Valkovič L, Pavlides M, Robson MD, Tunnicliffe EM. Hydration and glycogen affect T<sub>1</sub> relaxation times of liver tissue. *NMR in Biomedicine*. 2021;34:e4530. <https://doi.org/10.1002/nbm.4530>